

Improving EFTEM 3D Chemical maps by multivariant statistical analysis and iterative denoising

C. Messaoudi^{1,2}, N. Aschman^{1,2}, M. M. Lyra da Cunha^{1,2}, T. Oikawa³, C.O.S. Sorzano⁴ and S. Marco^{1,2}

1. Institut Curie, Centre de Recherche, Orsay, 91405 France.

2. INSERM, U759, Orsay, 91405 France.

3. JEOL Ltd., Akishima, Tokyo 196-8558, Japan.

4. Centro Nacional de Biotecnología, Univ. Autónoma de Madrid, Cantoblanco, Madrid, 28049 Spain.

cedric.messaoudi@curie.fr

Keywords: Tomography, EFTEM, 3D chemical mapping.

Electron tomography is becoming one of the most used methods for structural analysis at nanometric scale in biological and material sciences. Combined with chemical mapping, it provides qualitative and semiquantitative information on the distribution of chemical elements on a given sample. Due to the current milestones on obtaining 3D maps by EFTEM, the use of 3D chemical mapping is still not spread among the electron microscopy community. This complexity is associated to the absence of specialized software allowing the computation of maps when SNR is low. Moreover, data interpretation is complicated by the absence of efficient segmentation tools. Thus, specialized software to compute 3D maps by EFTEM needs to include optimized methods for series alignment, algorithms to improve SNR, different background subtraction models and methods to facilitate map segmentation.

Here we present software (EFTEM-TOMOJ), especially devoted for computation of EFTEM 3D Chemical maps. This software has been developed as a Java plug-in for the popular image analysis application ImageJ [1]. EFTEM-TomoJ proposes automatic image alignment based on multiscale methods and mutual information [2] allowing the use of images containing different types of information (for instance alignment of medium and high energy loss images with Z-loss or plasmon as reference); graphical tools for manual alignment; six different background subtraction laws (linear regression, power, exponential, polynomial of order two, log-polynomial of order 2, log-log polynomial of order two). Also, this package implements a noise filtering by image reconstitution based on multivariate statistical analysis to preserve signal while removing noise [3,4]. After computation of the background-subtracted tilt-series, the use of the TomoJ [5] imageJ plugin to calculate the 3D reconstruction results in a 3D map improved by the use of a new algorithm (BgART) recently implemented in TomoJ. BgART uses an initial ART/SIRT reconstructed volume to compute the grey level corresponding to the maximum value of the histogram. This value is used to discriminate between background and signal to improve the reconstructed volume in an iterative way.. Software interface is shown in Figure 1 and an example of application to the iron distribution after cytochemistry with cationized ferritin for anionic sites detection in the pathogenic fungi *Fonsecaea pedrosoi* comparing the results before and after use of MVA and BgART is shown in Figure 2.

[1] WS Rasband, ImageJ, U. S. National Institutes of Health, Bethesda, Maryland, USA, <http://imagej.nih.gov/ij/>, 1997-2011.

[2] JPW Pluim, JBA Maintz and MA Viergever, IEEE transactions on medical imaging **22** (2003), p. 986

[3] P Trebbia and N Bonnet, Ultramicroscopy **34** (1990), p.165

[4] C Quintana, S Marco, N Bonnet, C Risco, ML Gutierrez, A Guerrero and JL Carascosa, Micron **29** (1998), p. 297

[5] C Messaoudi, T Boudier, COS Sorzano and S Marco, BMC Bioinformatics **8** (2007), p. 288

[6] The authors want to thank S Rozental (Instituto de biofísica Carlos Chagas Filho, UFRJ, Brazil) for providing biological samples.

Figure 1. View of the EFTEM-TomoJ interface corresponding to alignment and map computation

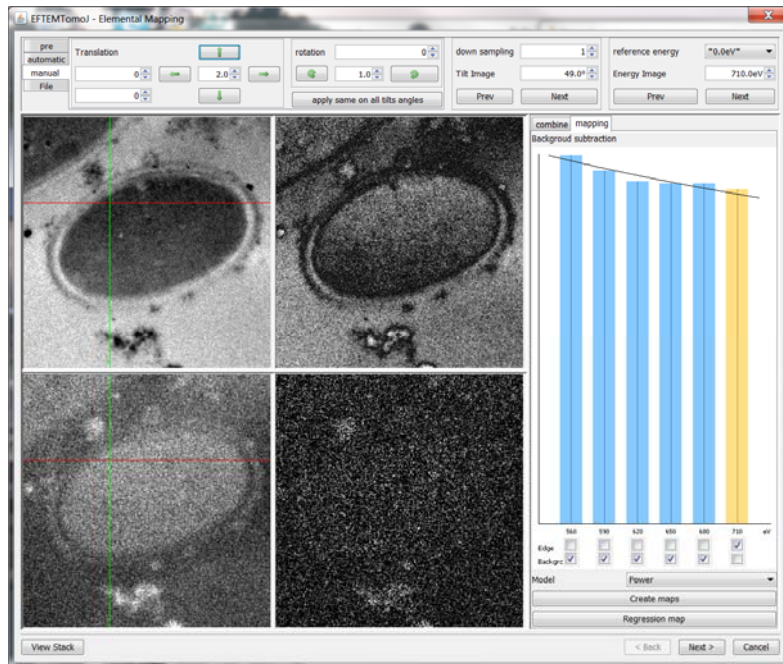


Figure 2. Comparison of central plane of 3D reconstructions of pathogenic fungi *Fonsecaea pedrosoi*. A) Z-loss reconstruction. Green arrow points to the cytoplasm where there should be no iron detected. Orange arrow points to a granule of iron. B) Iron distribution before use of MVA. Cytoplasm appears with specific iron signal when it should not. C) Iron distribution after use of MVA. Cytoplasm is now at the level of noise. D) Iron distribution after use of MVA and BgART. The noise is almost entirely removed allowing easy segmentation and/or 3D visualization.

